JM RAPIDS

Impulsive impact of a submerged body

Y.A. Semenov[1],†, Y.N. Savchenko[1] and G.Y. Savchenko[1]

[1]National Academy of Sciences of Ukraine, Institute of Hydromechanics, 8/4 Marii Kapnist Street, Kyiv 03057, Ukraine

An analytical solution of the impulsive impact of a cylindrical body submerged below a calm water surface is obtained by solving a free boundary problem. The shape of the cross-section of the body is arbitrary. The integral hodograph method is applied to derive the complex velocity potential defined in a parameter plane. The boundary-value problem is reduced to a Fredholm integral equation of the first kind in the velocity magnitude on the free surface. The velocity field, the impulsive pressure on the body surface and the added mass are determined in a wide range of depths of submergence for various cross-sectional shapes, such as a flat plate, a circular cylinder and a rectangle.

Key words: wave-structure interactions, surface gravity waves, contact lines

1. Introduction

The concept of impulse pressure goes back to the work of Lagrange (1783), in which he interpreted the product of the density times the velocity potential as the pressure impulse needed to suddenly impel a fluid from rest to its present velocity. It is worth mentioning the first work of Joukowskii (1884) on the impact between two spheres, one of which is half submerged in a liquid, which first dealt with the added mass. The impulse pressure concept received further development in the works of von Kármán (1929) and Wagner (1932) studying the initial stage of violent water impact flows with application to seaplane landing and ship slamming. Havelock studied the impulsively starting motion of a cylinder, with a constant velocity (Havelock 1949a) and a constant acceleration (Havelock 1949b), respectively. He applied a linearized free surface boundary condition and investigated the full time evolution of the free surface. Tyvand & Miloh (1995) studied an unsteady nonlinear free surface flow using the method of small-time-series expansion taking into consideration orders high enough to account for the leading gravitational effects on the surface elevation and to predict the hydrodynamic force acting on the cylinder. The related problem of water entry (water exit) of a circular cylinder was studied theoretically and experimentally by Greenhow (1983) and Greenhow & Yanbao (1987).

† Email address for correspondence: yuriy.a.semenov@gmail.com

The impulsive concept has been used to predict wave impacts on marine and coastal structures (Cooker & Peregrine 1995), ship slamming (Faltinsen 2005), the impulsive vertical motion of a body initially floating on a flat free surface (Iafrati & Korobkin 2005), dam-break flows (Korobkin & Yilmaz 2009), impulsive sloshing in containers and tanks (Tyvand & Miloh 2012), and drops that hit a solid or liquid surface in impulsive impact (Hjelmervik & Tyvand 2017). A solution based on the impulsive concept may lead to an infinite velocity where a free surface meets a solid body. In such cases, the impulse solution is used as an outer solution, which has to be matched with an inner solution in the vicinity of the contact line using the method of matched asymptotic expansion (King & Needham 1994; Iafrati & Korobkin 2005; Korobkin & Scolan 2006; Needham, Billingham & King 2007).

Mathematical models of impulse flows are based on the theory for an incompressible and irrotational flow, so that a velocity potential can be introduced. The free surface is assumed to be flat before the impact, and the potential on the free surface remains zero during the impact. The boundary value problem for the velocity potential can be written as follows:

$$\Delta \Phi' = 0 \tag{1.1}$$

in the fluid domain;

$$\Phi' = 0 \tag{1.2}$$

on the free surface;

$$\frac{\partial \Phi'}{\partial n} = -Un_y \tag{1.3}$$

on the body surface, where U is the velocity immediately after the impact, $\boldsymbol{n}$ is the outward normal to the body surface and n_y is its component in the y-direction; and

$$|\nabla \Phi'| \to 0, \quad x^2 + y^2 \to \infty, \tag{1.4}$$

which is the far-field condition.

In contrast to the previous studies, we consider the impulsive motion of a body fully submerged in a liquid. The motivation for this research comes from the naval hydrodynamics of high-speed hydrofoil craft, whose foil system may experience sudden vertical impacts caused by waves hitting the main body of the craft (Faltinsen 2005).

The impulsive pressure on the body, the velocity on the free surface and the associated added mass are determined in a wide range of depths of submergence and for various shapes, including a flat plate, a circular cylinder and a rectangle.

The study of the added mass is of interest in connection with the drift volume concept introduced in fluid mechanics by Darwin (1953). For a circular cylinder, he showed using the potential flow theory that the drift volume enclosed between the initial and the final positions of the body (at upstream and downstream infinity, respectively) is equal to the added-mass volume of the cylinder. Later, this was confirmed by Eames, Belcher & Hunt (1994) for a sphere. Peters *et al.* (2016) presented an experimental study for a disc impulsively set into motion on a plane oil–water interface. They showed that there exists a time window of universal behaviour of the entrained oil for various Froude numbers.

2. Boundary-value problem

A sketch of the physical domain is shown in figure 1(*a*). The body submerged below a calm free surface is symmetric about the *Y*-axis, and thus only half of the flow region is
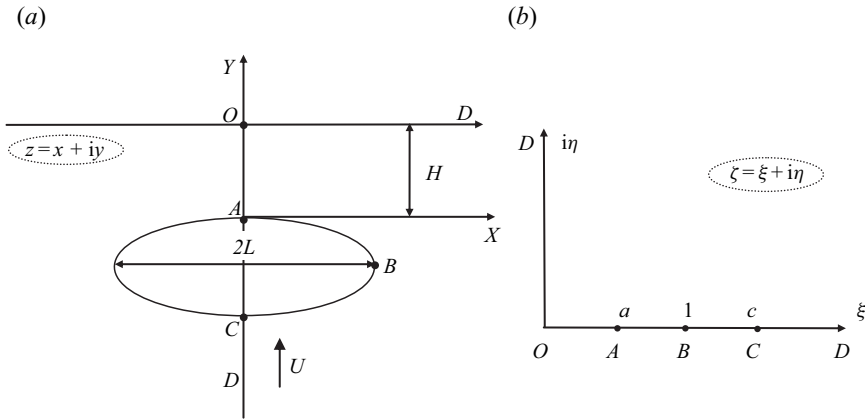
Figure 1. (*a*) Sketch of the physical plane, and (*b*) the parameter or ζ-plane.

considered. Before the impact, $t = 0$, the body and the liquid are at rest. At time $t = 0^+$ the body is suddenly set into motion with acceleration a directed downwards such that, during infinitesimal time interval $\Delta t \to 0$, the speed of the body reaches the value U. The problem of a rigid body moving in a fluid body is kinematically equivalent to the problem of a fluid body moving around a fixed rigid body with acceleration a at infinity. We define a non-inertial Cartesian system of coordinates XY attached to the body at point A, and an inertial system of coordinates $X'Y'$ in which the velocity of the liquid at infinity equals zero. The body is assumed to have an arbitrary shape, which can be defined by the slope of the body as a function of the arclength coordinate S, $\beta_b = \beta_b(S)$. The liquid is assumed to be ideal and incompressible. The flow starting from rest remains irrotational at subsequent times. Both gravity and surface tension are ignored.

We can introduce complex potentials $W(Z) = \Phi(X, Y) + i\Psi(X, Y)$ and $W'(Z) = \Phi'(X, Y) + i\Psi'(X, Y)$ with $Z = X + iY$. In these systems, the velocity fields are related as follows:

$$\frac{\mathrm{d}W}{\mathrm{d}Z} = \frac{\mathrm{d}W'}{\mathrm{d}Z} - iat, \tag{2.1}$$

where a is the acceleration, $0 < t < \Delta t$ and $\Delta t \to 0$. Integrating (2.1), we can find

$$W = W' - iatZ, \quad \frac{\partial W}{\partial t} = \frac{\partial W'}{\partial t} - iaZ, \quad \frac{\partial \Phi'}{\partial t} = \frac{\partial \Phi}{\partial t} - aY. \tag{2.2a–c}$$

By substituting the last equation into Bernoulli's equation

$$\frac{\partial \Phi'}{\partial t} + \frac{p}{\rho} + \frac{|V'|^2}{2} = \frac{p_a}{\rho}, \tag{2.3}$$

and integrating it over infinitesimal time interval $\Delta t \to 0$, one can obtain

$$P = \int_0^{\Delta t} p \, \mathrm{d}t = -\rho\Phi + \rho UY, \tag{2.4}$$

where p and P are the pressure and impulsive pressure, respectively, and $U = a\Delta t$. Here, $|V'| < \infty$ and p_a are the velocity magnitude and the pressure on the free surface, respectively, whose integrals over time interval $\Delta t \to 0$ tend to zero.

919 R4-3

We introduce dimensionless quantities normalized by U, L and ρ: $v = |V|/U$, $x = X/L$, $y = Y/L$, $h = H/L$ and $\phi(s) = \Phi(S)/(LU)$. The vertical impulse force F_y is obtained by integrating the impulse pressure over the body surface,

$$F_y = -2\rho L^2 U \int_{s_A}^{s_C} \phi(s) \cos(n, y) \, \mathrm{d}s - 2\rho U A = \rho m L^2 U, \qquad (2.5)$$

where s is the arclength coordinate along the body surface, s_A and s_C are the arclengths of points A and C, m is the added-mass coefficient and A is the cross-sectional area. The factor '2' accounts for the force acting on the part of the body symmetric about the y-axis. Owing to the symmetry of the body about the y-axis, the horizontal impulse force equals zero.

It is desired to determine the velocity potential $\phi(s)$ immediately after the impact.

3. Conformal mapping

To find the complex potential $w(z)$ directly is a challenge; therefore, we introduce an auxiliary parameter plane, or ζ-plane, as suggested by Michell (1890) and Joukovskii (1890). We formulate boundary-value problems for the complex velocity function, $\mathrm{d}w/\mathrm{d}z$, and for the derivative of the complex potential, $\mathrm{d}w/\mathrm{d}\zeta$, both defined in the ζ-plane. Then the derivative of the mapping function is obtained as $\mathrm{d}z/\mathrm{d}\zeta = (\mathrm{d}w/\mathrm{d}\zeta)/(\mathrm{d}w/\mathrm{d}z)$, and its integration provides the mapping function $z = z(\zeta)$ relating the coordinates in the parameter and physical planes.

We choose the first quadrant of the ζ-plane in figure 1(*b*) as the region corresponding to the fluid region in the physical plane (figure 1*a*). The conformal mapping theorem allows us to arbitrarily choose the locations of three points, which are points O at the origin ($\zeta = 0$), D (D') at infinity and B at $\zeta = 1$ (see figure 1*b*). The position of points A ($\zeta = a$) and C ($\zeta = c$) has to be determined from the solution of the problem and physical considerations.

3.1. *Expressions for the complex velocity and the derivative of the complex potential*

The body is considered to be fixed; therefore, the velocity direction and the slope of the body coincide. Besides, at this stage, we assume that the velocity magnitude on the free surface is a known function of the parameter variable, $v(\eta)$. Then the boundary-value problem for the complex velocity in the first quadrant of the parameter plane can be written as follows:

$$\chi(\xi) = \arg\left(\frac{\mathrm{d}w}{\mathrm{d}z}\right) = \begin{cases} -\beta_b(a) + \beta_0, & 0 \leq \xi \leq a, \\ -\beta_b(\xi), & a \leq \xi \leq c, \\ -\beta_b(c) - \beta_0, & c \leq \xi < \infty. \end{cases} \qquad (3.1)$$

$$v(\eta) = \left|\frac{\mathrm{d}w}{\mathrm{d}z}\right|_{\zeta = \mathrm{i}\eta}, \qquad 0 \leq \eta < \infty. \qquad (3.2)$$

where $\beta_0 = \pi/2$, $\beta_b(a) = \pi$ and $\beta_b(c) = 0$. Equation (3.1) satisfies the conditions: $\chi(\xi) = -\pi/2$ along the intervals OA and CD on the symmetry line, and $\chi(\xi) = -\beta_b(\xi)$ along the body. The argument of the complex velocity exhibits jumps $\Delta = -\pi/2$ at points A and C when we move along the boundary in the physical plane from point O to point D.

This boundary-value problem can be solved by applying the following integral formula (Semenov & Yoon 2009):

$$\frac{dw}{dz} = v_\infty \exp\left[\frac{1}{\pi}\int_0^\infty \frac{d\chi}{d\xi}\ln\left(\frac{\zeta+\xi}{\zeta-\xi}\right)d\xi - \frac{i}{\pi}\int_0^\infty \frac{d\ln v}{d\eta}\ln\left(\frac{\zeta-i\eta}{\zeta+i\eta}\right)d\eta + i\chi_\infty\right],$$
(3.3)

where $v_\infty = v(\eta)_{\eta\to\infty}$ and $\chi_\infty = \chi(\xi)_{\xi\to\infty}$. Substituting (3.1) and (3.2) into (3.3) and evaluating the first integral over the step change at points $\zeta = a$ and $\zeta = c$, we obtain

$$\frac{dw}{dz} = v_\infty \left(\frac{\zeta-a}{\zeta+a}\right)^{1/2}\left(\frac{\zeta-c}{\zeta+c}\right)^{1/2}$$
$$\times \exp\left[\frac{1}{\pi}\int_a^c \frac{d\beta_b}{d\xi}\ln\left(\frac{\zeta-\xi}{\zeta+\xi}\right)d\xi - \frac{i}{\pi}\int_0^\infty \frac{d\ln v}{d\eta}\ln\left(\frac{\zeta-i\eta}{\zeta+i\eta}\right)d\eta - i\beta_0\right].$$
(3.4)

It can be easily verified that for $\zeta = \xi$ the argument of the right-hand side of (3.4) is the function $-\beta_b(\xi)$, while for $\zeta = i\eta$ the modulus of (3.4) is the function $v(\eta)$, i.e. the boundary conditions (3.1) and (3.2) are satisfied. It can also be seen that the complex velocity function has zeros of order $1/2$, which correspond to the flow around a corner of angle $\pi/2$ at points A and C.

In order to derive the derivative of the complex potential, we have to analyse its behaviour. Before the impact, the free surface is flat, and it coincides with the x-axis (see figure 1a). The pressure along the free surface is constant. Then, as follows from the Euler equation, the velocity generated by the impact is perpendicular to the free surface where the pressure is constant, or the velocity is directed in the y-direction. Therefore, the x-component of the velocity is zero, and $dw = (dw/dz)\,dz = (v_x - iv_y)\,dx = -iv\,dx$. Thus, the free surface corresponds to the interval $(-\infty, 0)$ on the imaginary axis ψ in the w-plane. We have $\text{Im}(w) = 0$ along the line $OABCD$ due to the impermeability condition on the body ABC and the intervals OA and CD of the symmetry line. At the same time, $\text{Re}(w)$ changes from zero at point O to $-\infty$ at infinity D. Thus, the flow region in the physical plane corresponds to the third quadrant in the w-plane. They are related as $w = -K\zeta$, where K is a positive real number. Then one can obtain

$$\frac{dw}{d\zeta} = -K.$$
(3.5)

The simple form of the complex potential, $w(\zeta) = -K\zeta + w_O$, allows one to exclude the parameter ζ and obtain the solution in Kirchhoff's form, for which the complex velocity is a function of the complex potential. Here, w_O is the complex potential at point O.

The derivative of the mapping function is obtained by dividing (3.5) by (3.4), i.e.

$$\frac{dz}{d\zeta} = -K\left(\frac{\zeta+a}{\zeta-a}\right)^{1/2}\left(\frac{\zeta+c}{\zeta-c}\right)^{1/2}$$
$$\times \exp\left[\frac{1}{\pi}\int_a^c \frac{-d\beta_b}{d\xi}\ln\left(\frac{\zeta-\xi}{\zeta+\xi}\right)d\xi + \frac{i}{\pi}\int_0^\infty \frac{d\ln v}{d\eta}\ln\left(\frac{\zeta-i\eta}{\zeta+i\eta}\right)d\eta + i\beta_0\right].$$
(3.6)

The integration of this equation yields the mapping function $z = z(\zeta)$ relating the parameter and the physical planes. Equations (3.4) and (3.5) include the parameters a, c

and K and the functions $v(\eta)$ and $\beta_b(\xi)$, all to be determined from physical considerations and the kinematic boundary condition on the free surface and on the solid boundary *OABCD*.

3.2. *Body boundary conditions*

The arclengths between points A and B, s_{AB}, and between points B and C, s_{BC}, and the depth of submergence are determined as follows:

$$\int_a^1 \left|\frac{\mathrm{d}z}{\mathrm{d}\zeta}\right|_{\zeta=\xi} = s_{AB}, \quad \int_1^c \left|\frac{\mathrm{d}z}{\mathrm{d}\zeta}\right|_{\zeta=\xi} = s_{BC}, \quad \int_0^a \left|\frac{\mathrm{d}z}{\mathrm{d}\zeta}\right|_{\zeta=\xi} = h. \qquad (3.7a\text{--}c)$$

The unknown function $\beta_b(\xi)$ is determined from the following integro-differential equation:

$$\frac{\mathrm{d}\beta_b}{\mathrm{d}\xi} = \frac{\mathrm{d}\beta_b}{\mathrm{d}s}\left|\frac{\mathrm{d}z}{\mathrm{d}\zeta}\right|_{\zeta=\xi}, \qquad (3.8)$$

where $\beta_b(s)$ is the given function. Equation (3.8) is solved by iteration using $\mathrm{d}\beta_b/\mathrm{d}\xi$ in (3.6) known at the previous iteration.

3.3. *Free surface boundary conditions*

An impulsive impact is characterized by infinitesimally small time interval $\Delta t \to 0$ such that the position of the free surface does not change during the impact. From the Euler equations, it follows that the velocity generated by the impact is perpendicular to the free surface ($p = p_a$):

$$\arg\left(\frac{\mathrm{d}w}{\mathrm{d}z}\bigg|_{\zeta=i\eta}\right) = -\beta_0, \quad 0 \le \eta \le \infty. \qquad (3.9)$$

Taking the argument of the complex velocity from (3.4), we obtain the following integral equation in the function $\mathrm{d}\ln v/\mathrm{d}\eta$:

$$\int_0^\infty \frac{\mathrm{d}\ln v}{\mathrm{d}\eta} \ln\left|\frac{\eta'-\eta}{\eta'+\eta}\right| \mathrm{d}\eta' + \tan^{-1}\left(\frac{\eta}{a}\right) + \tan^{-1}\left(\frac{\eta}{c}\right)$$
$$+ \frac{2}{\pi}\int_a^c \frac{\mathrm{d}\beta_b}{\mathrm{d}\xi} \tan^{-1}\left(\frac{\eta}{\xi}\right) \mathrm{d}\xi = 0. \qquad (3.10)$$

Equation (3.10) is a Fredholm integral equation of the first kind with a logarithmic kernel. Its solution takes the form (see Appendix A)

$$v(\eta) = \sqrt{\eta^2 + a^2}\sqrt{\eta^2 + c^2}\exp\left(\frac{1}{\pi}\int_a^c \frac{\mathrm{d}\beta_b}{\mathrm{d}\xi}\ln(\eta^2 + \xi^2)\,\mathrm{d}\xi\right). \qquad (3.11)$$

Equations (3.7a–c), (3.8) and (3.10) form a closed system of equations in the parameters a, c and K and the functions $\beta_b(\xi)$ and $\ln v(\eta)$.

4. Results

The results presented below are shown in the system of coordinates related to the liquid at infinity. The velocity distribution on the free surface generated by the impulsive impact of
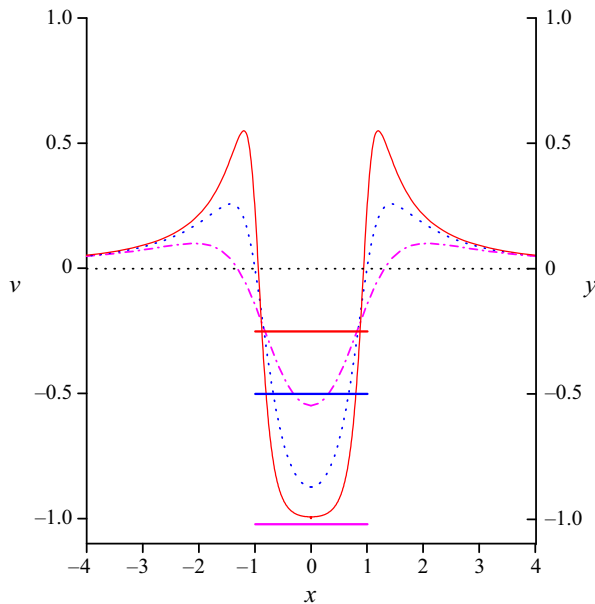
Figure 2. Velocity magnitude on the free surface (left axis) for various depths of submergence (right axis): $h = 0.25$ (red, solid line), 0.5 (blue, dotted line) and 1.0 (magenta, dot-dashed line).

a flat plate is shown in figure 2 for various depths of submergence. The position of the plate (right axis) is shown as a thick horizontal line. The colours of the plate and the associated velocity distribution are the same. After the impact, the plate gets a velocity equal to -1. At a relatively small depth of submergence, $h < 0.25$, the velocity of the liquid in front of the plate, $|x| < 1$, is close to -1, i.e. the plate entrains the liquid, and they move almost together. Outside of the plate, $|x| > 1$, the plate displaces the liquid, and it moves upwards, providing the balance of the liquid coming into and out of the flow region. The larger the depth of submergence of the plate, the smaller is the response of the free surface.

The velocity distribution along the free surface and the impulsive pressure versus the arclength coordinate s are shown for a circular cylinder in figures 3(*a*) and 3(*b*), respectively. The coordinates $s = 0$ and $s = \pi$ correspond to the top (point *A*) and the bottom (point *C*) of the cylinder. The bottom pressure is positive, and it depends only weakly on the depth of submergence. At the top of the cylinder, the pressure is negative, but it increases as the cylinder approaches the free surface.

The response of the free surface caused by the impulsive impact of a submerged rectangle is shown in figure 4 for depth $h = 0.25$ and various values of the side length b of the rectangle. For a small length, $b = 0.1$, the velocity distribution is close to that shown in figure 2 for a plate at depth $h = 0.25$. For larger lengths b, the velocity decreases, while the length of the free surface in the x-direction affected by the impact increases. Such behaviour provides a balance between the liquid moving into and out of the flow region.

The added-mass coefficients are shown in table 1 for various shapes of the body. For a flat plate, $m \to \pi/2$ as $h \to 0$, which agrees with the added mass for a flat plate floating on a free surface (von Kármán impact solution). For a large depth of submergence, $h = 50$, the effect of the free surface becomes negligible, and the coefficient of the added mass approaches the value corresponding to the added mass in an unbounded fluid domain. Greenhow & Yanbao (1987) presented Walton's analytical formula for the added mass of
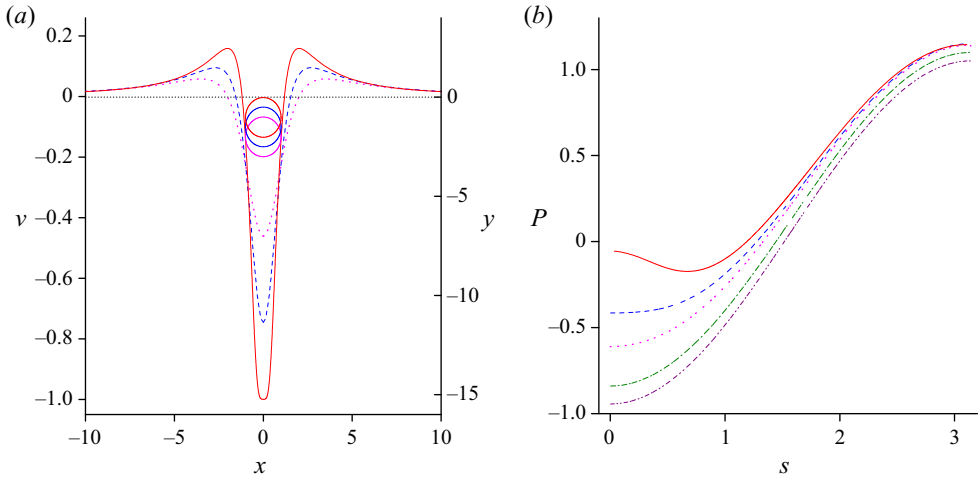
Figure 3. (*a*) Velocity along the free surface (left axis) and (*b*) impulsive pressure along the cylinder for various depths of submergence (right axis): $h = 0.02$ (red, solid line), 0.1 (blue, dashed line), 1.0 (magenta, dotted line), 3.0 (green, dot-dashed line) and 10.0 (purple, dot-dot-dashed line).
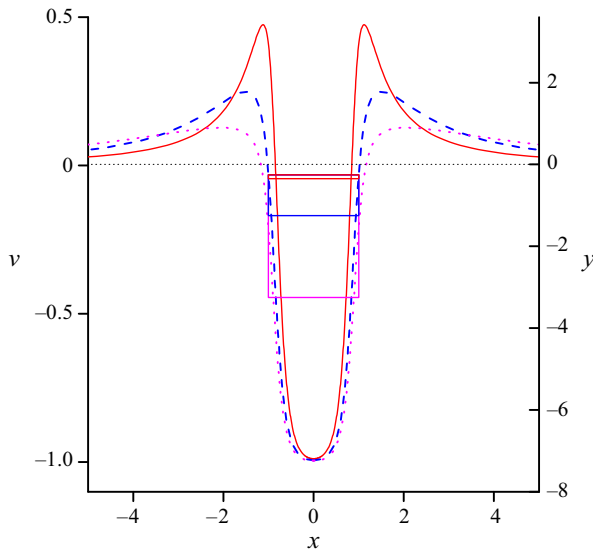

Figure 4. Velocity (left axis) along the free surface generated by the impact of a rectangle submerged at depth $h = 0.25$ and the position of the rectangle (right axis): side length $b = 0.1$ (red, solid line), $m = 2.272$; $b = 1.0$ (blue, dashed line), $m = 2.786$; and $b = 3$ (magenta, dotted line), $m = 3.241$. The top surface of the rectangles, $y = -h$, is the same, while the bottom surface, $y = -h - b$, is shown by the appropriate coloured line.

a submerged cylinder. An equivalent formula was proposed by Venkatesan (1985). The formulae contain elliptical integrals, and they are quite complicated for computations. Because of this, Greenhow & Yanbao (1987) proposed a polynomial approximation, which provides an accuracy within 2 %. The difference between the obtained results and those based on the approximation formula is also less than 2 %.

h	0	0.02	0.05	0.1	0.3	0.5	1	5	50	∞*
Plate	1.571	1.624	1.735	1.876	2.265	2.516	2.835	3.108	3.137	π
Square	—	2.993	3.011	3.048	3.292	3.552	4.024	4.667	4.754	4.754
Circle	—	2.064	2.111	2.162	2.370	2.531	2.777	3.104	3.141	π
Circle**	—	2.027	2.071	2.139	2.365	2.528	2.772	3.103	3.141	π

Table 1. Added-mass coefficient for various cross-sectional shapes of the cylinder and depths of submergence: *unbounded fluid domain; **approximate formula (Greenhow & Yanbao 1987).
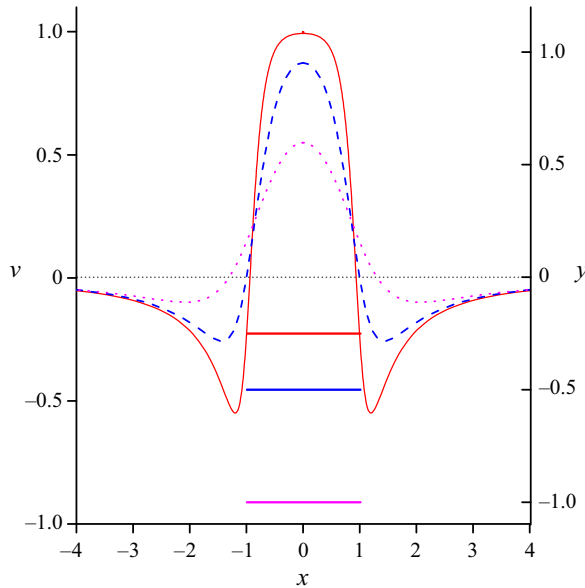

Figure 5. The same as in figure 2 but opposite (upward) direction of impact.

5. Upward impulsive impact

Here, we analyse how the direction of an impact on a submerged body affects the velocity field. In the system of coordinates attached to the body, a change of the impact direction results in a reversal of the velocity direction of the liquid at infinity and on the whole solid boundary, including the body and the symmetry line. Equation (3.1) will keep its form if we set values $\beta_0 = -\pi/2$, $\beta_b(a) = 0$ and $\beta_b(c) = -\pi$, or subtract π from $\chi(\xi)$ in (3.1). In this case, the expression for the complex velocity (3.4) keeps its form. The derivative of the complex potential is obtained from (3.5) if we change the sign of the expression. Thus, all the equations of the problem keep their form. Therefore, the velocity magnitude on the free surface (3.11) remains the same for both upward and downward impact directions.

In the system of coordinates related to the liquid, a change of the impact direction results in a reversal of the velocity direction on the free surface, while the magnitude of the velocity and the added-mass coefficients are identical to the case of downward impact. Figure 5 illustrates the velocity distribution on the free surface corresponding to an upward impact of the plate for the same depths of submergence as shown in figure 2 for a downward impact. The velocity distribution on the free surface near the plate edges predetermines flow separation from the plate edges in later times.

6. Conclusions

An analytical solution of the impulsive impact of a cylindrical body below an undisturbed free surface is found using the integral hodograph method. The cross-sectional shape of the body may be a polygon or an arbitrary smooth shape. The results are shown for a flat plate, a circular cylinder and a rectangle. The equation for the complex velocity includes the velocity magnitude on the free surface, whose analytic form has been determined.

The associated added masses are found as a function of the depth of submergence. As the depth of submergence tends to infinity, the added mass tends to the value corresponding to the added mass in an unbounded fluid domain.

It is shown that upward and downward impacts generate an identical magnitude of the velocity on the free surface and identical added-mass coefficients. However, the velocity direction is opposite. The obtained solution can be considered as a first-order solution in solving the problem using the method of small time series.

The presence of a free surface does not change the structure of the flow near the body, which determines the added mass. Therefore, we may expect that the obtained results will reflect real situations similar to those occurring in the case of an unbounded fluid domain.

Author ORCIDs.
Ⓓ Y.A. Semenov http://orcid.org/0000-0002-1228-9097;
Ⓓ G.Y. Savchenko http://orcid.org/0000-0001-7177-3228.

Appendix A

Let us consider a polygon inscribed in a given smooth boundary of the body. Let N_p be the number of sides of length l_i, the slope of which is β_{pi}. Let ξ_i, $i = 1, 2, \ldots, N_p$, be the points in the parameter region corresponding to the vertices of the polygon. Then the function $\beta_b(\xi)$ can be written explicitly as

$$\beta_b(\xi) = \beta_{bi}, \quad \xi_{i-1} < \xi \leq \xi_i, \quad i = 1, \ldots N_p, \tag{A1a,b}$$

where $\xi_0 = a$, $\xi_{N_p} = c$, $\beta_{p1} = \pi$ and $\beta_{Np} = 0$.

By substituting (A1a,b) into (3.4) and evaluating the integral over the step change in the function $\beta_b(\xi)$ at points $\xi = \xi_i$, we obtain the complex velocity for the polygon-shaped body

$$\frac{\mathrm{d}w}{\mathrm{d}z} = \left(\frac{\zeta - a}{\zeta + a}\right)^{1/2} \left(\frac{\zeta - c}{\zeta + c}\right)^{1/2} \prod_{i=1}^{N_p} \left(\frac{\zeta - \xi_i}{\zeta + \xi_i}\right)^{\Delta\beta_{pi}/\pi}$$

$$\times \exp\left[-\frac{\mathrm{i}}{\pi} \int_0^\infty \frac{\mathrm{d}\ln v}{\mathrm{d}\eta} \ln\left(\frac{\zeta - \mathrm{i}\eta}{\zeta + \mathrm{i}\eta}\right) \mathrm{d}\eta - \mathrm{i}\beta_0\right]. \tag{A2}$$

The free surface boundary condition (3.9) with the complex velocity (A2) leads to the integral equation

$$\int_0^\infty \frac{\mathrm{d}\ln v}{\mathrm{d}\eta} \ln\left|\frac{\eta' + \eta}{\eta' - \eta}\right| \mathrm{d}\eta' = f(\eta), \tag{A3}$$

where

$$f(\eta) = \tan^{-1}\left(\frac{\eta}{a}\right) + \tan^{-1}\left(\frac{\eta}{c}\right) + \frac{2}{\pi} \sum_{i=1}^{N_b} \Delta\beta_{bi} \tan^{-1}\left(\frac{\eta}{\xi_i}\right). \tag{A4}$$

By applying the following transformations (Polyanin & Manzhirov 1998):

$$\frac{\mathrm{d}\ln v}{\mathrm{d}\eta} = -\frac{2}{\pi^2}\frac{\mathrm{d}}{\mathrm{d}\eta}\int_{\eta}^{\infty}\frac{F(u)\,\mathrm{d}u}{\sqrt{u^2-\eta^2}}, \quad F(u) = \frac{\mathrm{d}}{\mathrm{d}u}\int_{0}^{u}\frac{pf(p)}{\sqrt{u^2-p^2}}\,\mathrm{d}p, \qquad (A5a,b)$$

the solution of the integral equation (A3) is obtained as

$$v(\eta) = \sqrt{\eta^2+a^2}\sqrt{\eta^2+c^2}\prod_{i=1}^{N_p}(\eta^2+\xi_i^{\,2})^{\Delta\beta_{bi}/\pi}. \qquad (A6)$$

By taking the limit of (A6) for $N_b \to \infty$ and using $\Delta\beta_{bi} = (\mathrm{d}\beta_b/\mathrm{d}\xi)_i\Delta\xi_i$, we obtain equation (3.11).

REFERENCES

COOKER, M.J. & PEREGRINE, D.H. 1995 Pressure-impulse theory for liquid impact problems. *J. Fluid Mech.* **297**, 193–214.

DARWIN, C. 1953 Note on hydrodynamics. *Math. Proc. Camb. Phil. Soc.* **49** (2), 342–354.

EAMES, I., BELCHER, S.E. & HUNT, J.C.R. 1994 Drift, partial drift and Darwin's proposition. *J. Fluid Mech.* **275**, 201–223.

FALTINSEN, O.M. 2005 *Hydrodynamics of High-speed Marine Vehicles*. Cambridge University Press.

GREENHOW, M. 1983 Nonlinear free surface effects: experiments and theory. *Tech. Rep.* 83-19. MIT, Department of Ocean Engineering.

GREENHOW, M. & YANBAO, L. 1987 Added masses for circular cylinders near or penetrating fluid boundaries-review, extension and application to water-entry, -exit and slamming. *Ocean Engng* **14** (4), 325–348.

HAVELOCK, T.H. 1949*a* The wave resistance of a cylinder started from rest. *Q. J. Mech. Appl. Maths* **2**, 325–334.

HAVELOCK, T.H. 1949*b* The resistance of a submerged cylinder in accelerated motion. *Q. J. Mech. Appl. Maths* **2**, 419–427.

HJELMERVIK, K.B. & TYVAND, P.A. 2017 Incompressible impulsive wall impact of liquid cylinders. *J. Engng Maths* **103**, 159–171.

IAFRATI, A. & KOROBKIN, A.A. 2005 Starting flow generated by the impulsive start of a floating wedge. *J Engng Maths* **51**, 99–125.

JOUKOWSKII, N.E. 1884 On impact of two spheres, one of which floats in liquid. *Mat. Otd. Novorossiiskogo Obshchestva Estestvoispytatelej* **5**, 43–48.

JOUKOVSKII, N.E. 1890 Modification of Kirchhoff's method for determination of a fluid motion in two directions at a fixed velocity given on the unknown streamline. *Math. Sbornik.* **15** (1), 121–278.

VON KÁRMÁN, T. 1929 The impact of seaplane floats during landing. *NACA Tech. Note* 321.

KING, A. & NEEDHAM, D. 1994 The initial development of a jet caused by fluid, body and free-surface interaction. Part 1. A uniformly accelerating plate. *J. Fluid Mech.* **268**, 89–101.

KOROBKIN, A. & YILMAZ, O. 2009 The initial stage of dam-break flow. *J. Engng Maths* **63**, 293–308.

KOROBKIN, A.A. & SCOLAN, Y.-M. 2006 Three-dimensional theory of water impact. Part 2. Linearized Wagner problem. *J. Fluid Mech.* **549**, 343–373.

LAGRANGE, J.-L. 1783 Memoire sur la theorie du mouvement des fluides. *Nouv. Mem. Acad. Sci. Berlin* **12**, 151–188.

MICHELL, J.H. 1890 On the theory of free stream lines. *Phil. Trans. R. Soc. Lond.* A **181**, 389–431.

NEEDHAM, D., BILLINGHAM, J. & KING, A. 2007 The initial development of a jet caused by fluid, body and free-surface interaction. Part 2. An impulsively moved plate. *J. Fluid Mech.* **578**, 67–84.

NEWMAN, J.N. 1977 *Marine Hydrodynamics*. The MIT Press.

PETERS, I.R., MADONIA, M., LOHSE, D. & VAN DER MEER, D. 2016 Volume entrained in the wake of a disk intruding into an oil-water interface. *Phys. Rev. Fluids* **1**, 033901.

POLYANIN, A.D. & MANZHIROV, A.V. 1998 *Hand Book of Integral Equations*. CRC.

SEMENOV, Y.A. & YOON, B-S. 2009 Onset of flow separation for the oblique water impact of a wedge. *Phys. Fluids* **21**, 112103.

TYVAND, P.A. & MILOH, T. 1995 Free-surface flow due to impulsive motion of a submerged circular cylinder. *J. Fluid Mech.* **286**, 67–101.

TYVAND, P.A. & MILOH, T. 2012 Incompressible impulsive sloshing. *J. Fluid Mech.* **708**, 279–302.

VENKATESAN, S.K. 1985 Added mass of two cylinders. *J. Ship Res.* **29** (4), 234–240.

WAGNER, H. 1932 Über Stoß und Gleitvorgänge an der Oberfläche von Flüssigkeiten. *Z. Angew. Math. Mech.* **12**, 192–215.